



rijksuniversiteit
groningen

faculteit Wiskunde en
Natuurwetenschappen

On the theory of collisional orbits in the two center problem.

Bacheloronderzoek Wiskunde en Natuurkunde

Januari 2014

Student: E. Verhaar

Eerste Begeleider: H. Waalkens

Tweede Begeleider: E. van der Giessen

Abstract

The two center problem or *Euler's three body problem*, concerns motion of a mass around two fixed centers of attraction. In this paper, we will specifically look at one-parameter families of non-collisional orbits in the planar case of the two center problem. The system is integrable and hence, by the Liouville-Arnold theorem, the phase space is foliated by invariant 2-tori. To find these 2-tori we make use of elliptic coordinates. Orbits lying on a 2-torus and are either periodic or quasi-periodic. Quasi-periodic orbits will densely fill the torus, so no one-parameter families of non-collisional orbits exist. We will show that in the case of periodic orbits, there can be at most two distinct collisional orbits and there exist one-parameter families of non-collisional orbits.

1 Introduction

The two center problem is a special case of the more general three body problem. The three body problem consists of describing the motion of three bodies that exert an attracting force on each other. In the two center problem, two of these three bodies, the *centers*, are fixed in space. The problem now reduces to describing the motion of a particle in the force field formed by the two centers. This problem was first considered in 1760 by Leonhard Euler and is also referred to as *Euler's three body problem*. Euler was already able to integrate the equations of motion for the two-dimensional planar system. Later, Jacobi used elliptic integrals for this [1].

Applications of the two center problem include molecular physics and celestial mechanics. The problem is for example applicable to the hydrogen ion, which consists of two atom nuclei and one electron. This started off with Pauli in 1922 [2]. He used the Born-Oppenheimer approximation, in which the positions of the nuclei are fixed, and he was therefore considering the ion as a system with two centers. Later, Strand and Reinhardt [3] continued Pauli's work, also rectifying the flaw in Pauli's work where he stated that the hydrogen molecular ion could only exist in a metastable state. Another interesting application of the two center problem is the collision of ions with electrons, in which an electron is accelerated by shortly following a figure-eight trajectory around a pair of ions [4, 5]. An example for use of the two center problem in celestial mechanics is the description of the motion of a body in the vicinity of two black holes [6, 7].

In 2004, Waalkens et al. [8] studied foliation and action-angle variables of the two center problem. In the current study we will use the same approach as Waalkens et al., but we will focus on finding non-collisional orbits. More specifically, we will look for one-parameter families of such orbits.

In the three-dimensional problem, there are three constants of motion (CoMs): the total energy, the angular momentum and another, less obvious quantity [9]. The conservation of angular momentum follows from rotational symmetry around the axis through the two centers. For any nonzero value of this angular momentum, conservation of it prevents the moving particle to collide with one of the two centers. Therefore, in this paper, we will only look at the two-dimensional planar case with zero angular momentum, in which collisions can occur.

In two dimensions, motion in the two center problem is separable in elliptic coordinates. These coordinates are therefore the natural ones to use. We will show the separation in chapter 2, after a formulation of the Hamiltonian of the system in Cartesian coordinates.

For the planar two center problem, there are four types of motion as classified by Charlier in 1902 [10], and later more systematically by Deprit [11]. We will focus on the so called *lemniscate* trajectories, for which collisions with both centers can occur.

For such trajectories, only certain values of the CoMs are allowed. In chapter 3 we will derive what these values are and therefore, what initial conditions are allowed to have lemniscate motion.

In the event of a collision of the moving particle with one of the centers, velocity and generalized momenta will blow up to infinity. So numerical integration of the equations of motion of collisional orbits will not be accurate. We can, however, use a scaling of time introduced by Thiele and Burrau [12, 13] to regularize collisions. We will do this in section 2.2.

After separation, the motion can be described as a superposition of an anharmonic oscillator and a pendulum [14], each with a period that depends only on the CoMs. So by choosing the CoMs in a way that the ratio of these periods (the so called *winding number*) is a rational number, the total movement will be periodic, independent of the initial conditions. For periodic movement we can then determine if the orbit is collisional or not. We will do this in chapter 5, by classifying the collisional orbits by their winding number.

As mentioned before, in this thesis we will be looking for one-parameter families of non-collisional periodic orbits of lemniscate type. In chapter 5, we shall show that there are indeed such one-parameter families. All orbits belonging to these families cross the line connecting the two centers and the varying parameter is the position where this line is crossed, while the CoMs remain unchanged.

The outline of the paper is as follows. We start off in chapter 2 by introducing the Hamiltonian of the problem, introducing elliptic coordinates and finding the CoMs. In chapter 3 we will deduce what conditions the values of these CoMs must fulfil to have lemniscate motion. In 4 we use the Liouville-Arnold theorem to express the winding number in terms of the CoMs. And finally, in chapter 5 we look at periodic orbits.

2 Hamiltonian of the two center problem

We will consider the motion of a particle with mass m in the field created by two fixed attracting centers \mathbf{f}_1 and \mathbf{f}_2 . Using Cartesian coordinates, we can choose the origin and orientation of the axes in such a way that the centers are located at the points $\mathbf{f}_{1,2} = (0, 0, \mp a)$ in the (x, y, z) -space, with a some positive real number. This way, \mathbf{f}_1 is the lower and \mathbf{f}_2 is the upper center.

The potential energy of the free particle is inversely proportional to the distances to either of the two attracting centers, as is the case in, for example, gravitational or electronic attraction. The Hamiltonian for this system is given by

$$H = \frac{\mathbf{p}^2}{2m} - \frac{\mu_1}{r_1} - \frac{\mu_2}{r_2},$$

where \mathbf{p} is the momentum-vector, r_1 and r_2 are the distances to \mathbf{f}_1 and \mathbf{f}_2 and μ_1 and μ_2 are the respective constants of proportionality, which are positive in the case of attracting centers.

The system can be simplified by taking the appropriate units for length and time. First, we can scale the unit of length to a so that the centers are at the points $\mathbf{f}_{1,2} = (0, 0, \mp 1)$. Then we take time in units of $\sqrt{ma^3/(\mu_1 + \mu_2)}$. This way, the unit for momentum is $\sqrt{m(\mu_1 + \mu_2)/a}$ and that of energy is $(\mu_1 + \mu_2)/a$. With this scaling, the Hamiltonian becomes

$$H = \frac{\mathbf{p}^2}{2} - \frac{\mu}{r_1} - \frac{1 - \mu}{r_2}, \quad (1)$$

where $\mu = \mu_1/(\mu_1 + \mu_2)$.

Instead of Cartesian coordinates (x, y, z) , we can also analyse the system in cylindrical coordinates $(\rho, \phi, z) \in \mathbb{R}^+ \times S^1 \times \mathbb{R}$, with transformation

$$x = \rho \cos \phi, \quad (2)$$

$$y = \rho \sin \phi, \quad (3)$$

$$z = z, \quad (4)$$

and generalized momenta (which can be obtained from taking the partial derivative of the Lagrangian with respect to the velocities $\dot{\rho}$, $\dot{\phi}$ and \dot{z} [15]).

$$p_\rho = \dot{\rho}, \quad (5)$$

$$p_\phi = \rho^2 \dot{\phi}, \quad (6)$$

$$p_z = \dot{z}. \quad (7)$$

This transformation has a singularity at $\rho = 0$.

In the cylindrical coordinates the Hamiltonian (1) becomes

$$H = \frac{p_\rho^2 + p_\phi^2/\rho^2 + p_z^2}{2} - \frac{\mu}{r_1} - \frac{1-\mu}{r_2}. \quad (8)$$

Since H is independent of ϕ , the quantity p_ϕ is a constant of motion:

$$\dot{p}_\phi = -\frac{\partial H}{\partial \phi} = 0. \quad (9)$$

This constant of motion is the angular momentum about the z -axis $l = \rho^2 \dot{\phi} = p_\phi$, so

$$\dot{\phi} = \frac{l}{\rho^2}. \quad (10)$$

For $l \neq 0$, the centrifugal repulsion dominates the attraction for small ρ . So in that case, ρ will always be greater than zero and the free particle will never collide with one of the centers. In the rest of the article we will focus on the planar case $l = 0$, for which trajectories can be collisional, and look for non-collisional orbits there.

In the case of $l = p_\phi = 0$, the motion resulting from (8) is restricted to a plane. For the rest of the paper, we choose the orientation of the axes such that all motion is in the (x, z) -plane. The configuration space is $Q_2 = \mathbb{R}^2$.

2.1 Elliptic coordinates

We can separate the remaining two-dimensional problem by introducing elliptic coordinates $(\xi, \eta) \in [1, \infty) \times [-1, 1]$, defined by

$$\xi = \frac{1}{2} \left(\sqrt{x^2 + (z+1)^2} + \sqrt{x^2 + (z-1)^2} \right) \quad (11)$$

$$\eta = \frac{1}{2} \left(\sqrt{x^2 + (z+1)^2} - \sqrt{x^2 + (z-1)^2} \right). \quad (12)$$

That is, ξ is the mean of the distances between the particle and either of the two centers and η is the difference between these distances divided by 2. The transformation from (ξ, η) to (x, z) is given by:

$$x = \pm \sqrt{(\xi^2 - 1)(1 - \eta^2)}, \quad (13)$$

$$z = \xi\eta. \quad (14)$$

In the (x, z) plane the lines $\xi = \text{constant}$ form ellipses with the two centers \mathbf{f}_1 and \mathbf{f}_2 as foci. Larger values for ξ correspond to larger ellipses (ξ corresponds to the semi-major axis of the ellipse). The line $\xi = 1$ consists of the line segment connecting the two centers. The lines $\eta = \text{constant}$ form hyperbolas, also with \mathbf{f}_1 and \mathbf{f}_2 as foci. The line $\eta = -1$ corresponds to the part of the z -axis below $z = -1$ and the line $\eta = 1$ to the part of the z -axis above $z = 1$.

With the use of the (ξ, η) -coordinates, only half of the (x, z) -plane is covered, dependent on the sign used in equation (13). If we set $\xi = \cosh \lambda$ and $\eta = \sin \nu$ then we obtain

$$x = \sqrt{(\cosh^2 \lambda - 1)(1 - \sin^2 \nu)} = \sinh \lambda \cos \nu, \quad (15)$$

$$z = \cosh \lambda \sin \nu. \quad (16)$$

Now, the transformation from $(\lambda, \nu) \in \mathbb{R} \times S^1[-\pi, \pi]$ to $(x, z) \in \mathbb{R}$ is surjective, but not injective. For every point (x, z) , with exception of \mathbf{f}_1 and \mathbf{f}_2 , there are two possible (λ, ν) pairs, one with $\lambda \geq 0$ and $\nu \in (-\frac{\pi}{2}, \frac{\pi}{2})$ and one with $\lambda \leq 0$ and $\nu \in (-\pi, -\frac{\pi}{2}) \cup (\frac{\pi}{2}, \pi)$. The operation $(\lambda, \nu) \rightarrow (-\lambda, \pi - \nu)$ yields the same point in the (x, z) -plane. So the cylinder $\bar{Q}_2 = \{(\lambda, \nu) \in \mathbb{R} \times S^1[-\pi, \pi]\}$ is a two-sheeted cover for the configuration space Q_2 , with branch points at the two centers.

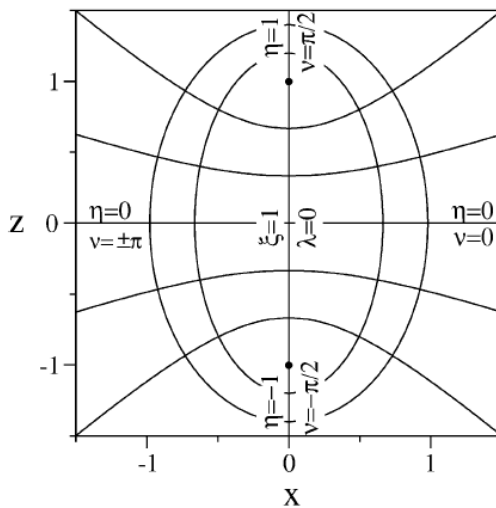


Figure 1: Elliptic coordinates [8]

2.2 Regularization of collisions

In the coordinates (λ, ν) the generalized momenta are

$$p_\lambda = (\cosh^2 \lambda - \sin^2 \nu) \dot{\lambda}, \quad (17)$$

$$p_\nu = (\cosh^2 \lambda - \sin^2 \nu) \dot{\nu}, \quad (18)$$

and the Hamiltonian becomes

$$\begin{aligned} H &= \frac{p_\lambda^2 + p_\nu^2}{2(\cosh^2 \lambda - \sin^2 \nu)} - \frac{\mu}{\cosh \lambda + \sin \nu} - \frac{1 - \mu}{\cosh \lambda - \sin \nu} \\ &= \frac{\frac{1}{2}(p_\lambda^2 + p_\nu^2) - (1 - 2\mu) \sin \nu - \cosh \lambda}{\cosh^2 \lambda - \sin^2 \nu}. \end{aligned} \quad (19)$$

Hamiltons equations now give us the equations of motion in elliptic coordinates:

$$\frac{dp_\lambda}{dt} = -\frac{\partial H}{\partial \lambda} = \frac{\sinh \lambda + 2H \cosh \lambda \sinh \lambda}{\cosh^2 \lambda - \sin^2 \nu}, \quad (20)$$

$$\frac{d\lambda}{dt} = \frac{\partial H}{\partial p_\lambda} = \frac{p_\lambda}{\cosh^2 \lambda - \sin^2 \nu}, \quad (21)$$

$$\frac{dp_\nu}{dt} = -\frac{\partial H}{\partial \nu} = \frac{(1 - 2\mu) \cos \nu - 2H \sin \nu \cos \nu}{\cosh^2 \lambda - \sin^2 \nu}, \quad (22)$$

$$\frac{d\nu}{dt} = \frac{\partial H}{\partial p_\nu} = \frac{p_\nu}{\cosh^2 \lambda - \sin^2 \nu}. \quad (23)$$

These equations of motion are regular everywhere on the cylinder \bar{Q}_2 , except at the points $(\lambda, \nu) = (1, \mp \frac{\pi}{2})$, where $(\cosh^2 \lambda - \sin^2 \nu) = 0$. These singularity points result from the two centers \mathbf{f}_1 and \mathbf{f}_2 . To regularize collisions, we scale the time by introducing τ , with

$$dt = (\cosh^2 \lambda - \sin^2 \nu) d\tau. \quad (24)$$

Using this scaled time, the equations of motion are regular everywhere and can be integrated:

$$\frac{dp_\lambda}{d\tau} = \frac{dp_\lambda}{dt} \frac{dt}{d\tau} = \sinh \lambda + 2H \cosh \lambda \sinh \lambda, \quad (25)$$

$$\frac{d\lambda}{d\tau} = \frac{d\lambda}{dt} \frac{dt}{d\tau} = p_\lambda, \quad (26)$$

$$\frac{dp_\nu}{d\tau} = \frac{dp_\nu}{dt} \frac{dt}{d\tau} = (1 - 2\mu) \cos \nu - 2H \sin \nu \cos \nu, \quad (27)$$

$$\frac{d\nu}{d\tau} = \frac{d\nu}{dt} \frac{dt}{d\tau} = p_\nu. \quad (28)$$

An interesting result of the time scaling, is that the new equations of motion are separated in elliptic coordinates. Of the four equations of motion, two equations only depend on λ and its derivatives, while the other two only depend on ν and its derivatives.

2.3 Constants of motion

The total energy is a conserved quantity, so the Hamiltonian is a constant of motion. We will denote the numeric value of H by h . The time scaling can be applied on equation (19) by introducing the adjusted Hamiltonian

$$\begin{aligned} \bar{H} &= (H - h) \frac{dt}{d\tau} \\ &= \frac{1}{2}(p_\lambda^2 + p_\nu^2) - (1 - 2\mu) \sin \nu - \cosh \lambda - h(\cosh^2 \lambda - \sin^2 \nu), \end{aligned} \quad (29)$$

and consider the level sets $H = h$. On these level sets $\bar{H} = 0$ and equation (29) can be rewritten as

$$-\frac{1}{2}p_\lambda^2 + H \cosh^2 \lambda + \cosh \lambda = \frac{1}{2}p_\nu^2 + H \sin^2 \nu - (1 - 2\mu) \sin \nu. \quad (30)$$

Since the left side of equation (30) does not depend on ν and the right side does not depend on λ , both sides must be constant. This separation thus gives another constant of motion, which we will denote by G , and its numerical value by g . In Cartesian coordinates G takes the form

$$G = H + \frac{1}{2}(\mathbf{L}^2 - p_x^2 - p_y^2) + (z + 1) \frac{\mu}{r_1} - (z - 1) \frac{1 - \mu}{r_2}, \quad (31)$$

where \mathbf{L} is the angular momentum about the origin. At the end of section 4.2.3 we will try to give a qualitative interpretation of the quantity G .

Using equations (25) and (27), we have

$$-g = \frac{1}{2}\lambda^2 - h \cosh^2 \lambda - \cosh \lambda \quad (32)$$

$$g = \frac{1}{2}\nu^2 + H \sin^2 \nu - (1 - 2\mu) \sin \nu. \quad (33)$$

These equations represent an anharmonic oscillator in λ and pendulum in ν .

3 Motion characteristics

3.1 Lemniscate motion

In this paper, we will concentrate on lemniscate motion. This is the motion for which the trajectory of the free particle crosses the line $\lambda = 0$ connecting the two centers and ν either increases or decreases monotonically on $S^1[-\pi, \pi]$. An example of a lemniscate trajectory is given in figure 2. In contrast to lemniscate motion, there are also *satellite* motion, in which the moving particle orbits around only one of the centers, and *planetary* motion, in which the moving particle orbits both centers but never crosses the line segment in between. In the current section, we will be looking for those combinations of h and g , the numerical values of H and G , for which the motion is of lemniscate type. We also require the motion to be bounded, so $h < 0$.

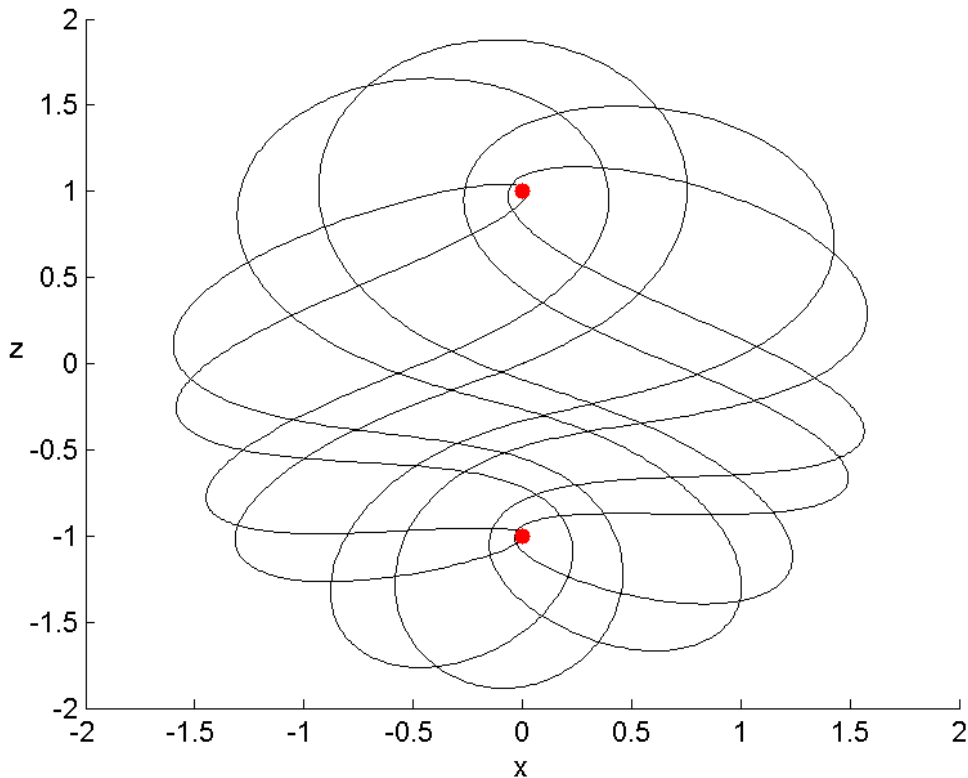


Figure 2: Periodic lemniscate motion for the case $\mu = \frac{1}{3}$, with $(h, g) = (0.5, 0.105)$.

To determine what values for h and g allow for lemniscate motion, we look at the squared momenta

$$p_\lambda^2 = 2h \cosh^2 \lambda + 2 \cosh \lambda - 2g, \quad (34)$$

$$p_\nu^2 = -2h \sin^2 \nu + 2(1 - 2\mu) \sin \nu + 2g. \quad (35)$$

For classically allowed motion, we require these squared momenta to be non-negative. Equation (34), together with the requirement that an open interval in λ containing $\lambda = 0$ is allowed, leads to the condition

$$g < h + 1. \quad (36)$$

To allow ν to be any value on $[-\pi, \pi]$, the right hand side of equation (35) has to be positive on this whole interval. To find the appropriate conditions for h and g , we first make sure that the right side of (35) is positive for at least the value $\nu = 0$. Then it suffices to make sure that it attains its sign on the whole interval $\nu \in [-\pi, \pi]$. Setting $\nu = 0$ in equation (35) gives the condition

$$g > 0. \quad (37)$$

Now, we substitute η for $\sin \nu$ in equation (35) and then look for real roots of p_ν^2 as a function of η . We require these to either not exist, or lie outside the interval $[-1, 1]$. This way, p_ν^2 remains positive for all possible values of ν . So we consider

$$p_\nu^2 = -2h\eta^2 + 2(1 - 2\mu)\eta + 2g. \quad (38)$$

The roots of the polynomial on the right hand side are

$$\eta_{\mp} = \frac{1 - 2\mu}{2h} \mp \sqrt{\frac{g}{h} + \frac{(1 - 2\mu)^2}{4h^2}}. \quad (39)$$

If the discriminant is negative, so when

$$\frac{g}{h} + \frac{(1 - 2\mu)^2}{4h^2} < 0,$$

no real roots exist. This comes down to (recall that h is negative)

$$g > \frac{-(1 - 2\mu)^2}{4h}, \quad (40)$$

in which case also equation (37) is satisfied. When

$$g \leq \frac{-(1 - 2\mu)^2}{4h}, \quad (41)$$

real roots of (38) exist.

When real roots exist, we need to make sure that they lie outside the interval $[-1, 1]$. We note that the parabolic graph of the quadratic function from equation (38) opens upward, and that as a result the part between the roots is negative. We therefore require the roots to lie at the same side outside the η -interval $[-1, 1]$. Since η_- is always negative, we require $\eta_+ < -1$. So

$$\frac{1 - 2\mu}{2h} + \sqrt{\frac{g}{h} + \frac{(1 - 2\mu)^2}{4h^2}} < -1,$$

which requires

$$h > \mu - \frac{1}{2}; \quad (42)$$

$$g > h + 1 - 2\mu. \quad (43)$$

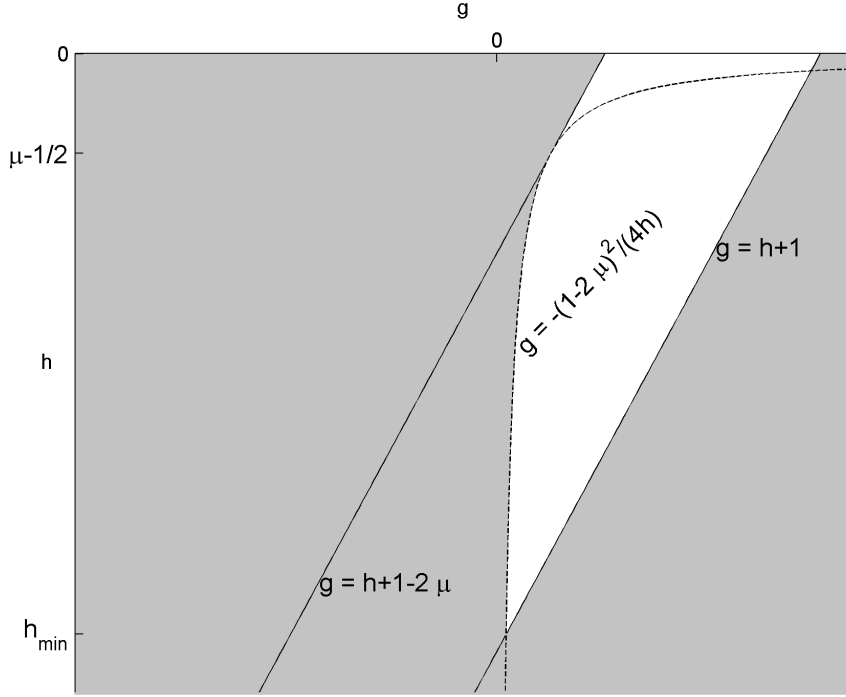


Figure 3: The (h, g) -plane. The white area represents motion of lemniscate type for $\mu = 1/3$.

To summarize, for lemniscate motion we require

$$g < h + 1 \quad (44)$$

and either

$$g > \frac{-(1 - 2\mu)^2}{4h} \quad (45)$$

or, if (45) does not hold,

$$h > \mu - \frac{1}{2} \quad (46)$$

$$g > \max\{0, h + 1 - 2\mu\} \quad (47)$$

These conditions give a region in the (h, g) plane for which the motion is of lemniscate type, which is depicted in figure 3. The boundary points of this region correspond to stationary points in either one of the coordinates λ or ν . From figure 3 it can be seen that there is a minimum value for h for lemniscate motion, that results from the combination of conditions (44) and (45). This minimum occurs at the lower intersection of the curves $g = h + 1$ and $g = -(1 - 2\mu)^2 / (4h)$, which is at

$$h_{\min} = -1/2 - \sqrt{\mu(1 - \mu)}. \quad (48)$$

3.2 Turning points

For bounded motion λ can only take on values below or equal to a certain λ_{\max} . The motion is restricted to the closed region bounded by the ellipse at $\lambda = \lambda_{\max}$, and points on this ellipse are turning points for the motion in λ . The value of λ_{\max} can be obtained by setting $p_\lambda = 0$ in equation (34):

$$2h \cosh^2 \lambda_{\max} + 2 \cosh \lambda_{\max} - 2g = 0, \quad (49)$$

or, substituting $\xi_{\max} = \cosh \lambda_{\max}$:

$$2h \xi_{\max}^2 + 2\xi_{\max} - 2g = 0. \quad (50)$$

This gives

$$\xi_{\max} = -\frac{1}{2h} + \sqrt{\frac{g}{h} + \frac{1}{4h^2}} \quad (51)$$

and accordingly

$$\lambda_{\max} = \cosh^{-1}\left(-\frac{1}{2h} + \sqrt{\frac{g}{h} + \frac{1}{4h^2}}\right). \quad (52)$$

We will use this result in the next section to find the action-coordinates.

4 Liouville-Arnold Theorem

In this paper, we will be looking for non-collisional orbits. To do so, we make use of the Liouville-Arnold theorem, which states the following [16]:

Theorem 1 (Liouville-Arnold). *Let M be a $2n$ -dimensional phase-space with local coordinates (p_j, q_j) , $j = 1, \dots, n$. And let $f_1, f_2, \dots, f_n : M \rightarrow \mathbb{R}$ be independent constants of motion, with f_1 the Hamiltonian H , that are in involution (that is, the Poisson brackets $\{f_i, f_j\} = \sum_{k=1}^n \frac{\partial f_i}{\partial q_k} \frac{\partial f_j}{\partial p_k} - \frac{\partial f_i}{\partial p_k} \frac{\partial f_j}{\partial q_k}$ vanish for all $i, j = 1, \dots, n$). Let*

$$M_f := \{(p, q) \in M; f_k(p, q) = c_k\}, \quad c_k = \text{constant}, \quad k = 1, \dots, n. \quad (53)$$

Then M_f is an n -dimensional manifold if (c_1, \dots, c_n) is a regular value of $(f_1, f_2, \dots, f_n) : M \rightarrow \mathbb{R}^n$.

If M_f is compact and connected, then it is diffeomorphic to an n -dimensional torus

$$T^n = \overbrace{S^1 \times S^1 \times \dots \times S^1}^{n \text{ times}}.$$

Furthermore, there exist action-angle coordinates $I_1, \dots, I_n, \phi_1, \dots, \phi_n$, such that the angular coordinates ϕ_k are coordinates on the torus T^n , and the actions I_k are constants of motion. The Hamiltonian can be expressed as a function of the actions only, so

$$H = H(I_1, \dots, I_n). \quad (54)$$

The equations of motion are

$$\dot{I}_k = -\frac{\partial H}{\partial \phi_k} = 0, \quad (55)$$

$$\dot{\phi}_k = \frac{\partial H}{\partial I_k} = \omega_k(I_1, \dots, I_n), \quad (56)$$

where the ω_k 's are called the frequencies. Because the frequencies depend on the (constant) I_k 's only, they are also constants of motion.

In the case of the two center problem, there are two degrees of freedom and the phase space is four-dimensional. We can set $(f_1, f_2) = (H, G)$ and $(c_1, c_2) = (h, g)$. Then M_f is the two-dimensional level surface consisting of all allowed points in phase space under the condition $(H, G) = (h, g)$.

4.1 Actions

In general, the action coordinates can be obtained by

$$I_k = \frac{1}{2\pi} \oint_{\Gamma_k} \sum_j p_j dq_j \quad (57)$$

where the Γ_k 's are independent cycles in phase space. We can use the separated coordinates λ and ν to get the 'natural' actions I_λ and I_ν . The independent cycles are then the paths in the phase space that result by holding respectively ν and λ constant on M , so that either $d\nu = 0$ or $d\lambda = 0$. These paths correspond to the phase diagrams of each separated coordinate. Equation (57) becomes

$$I_s = \frac{1}{2\pi} \oint p_s ds, \quad (58)$$

where s is either λ or ν and the integral is taken over one cycle in the two dimensional (s, p_s) phase plane. We will now separately consider I_λ and I_ν .

Using equation (34) we can plot the closed path for λ in a phase diagram, as done in figure 4. By symmetry about both the λ and the p_λ axes, the path can be divided into four equivalent parts and the action I_λ can be computed by

$$I_\lambda = \frac{2}{\pi} \int_0^{\lambda_{\max}} p_\lambda d\lambda, \quad (59)$$

where we can use the (positive) square root of equation (34) as p_λ .

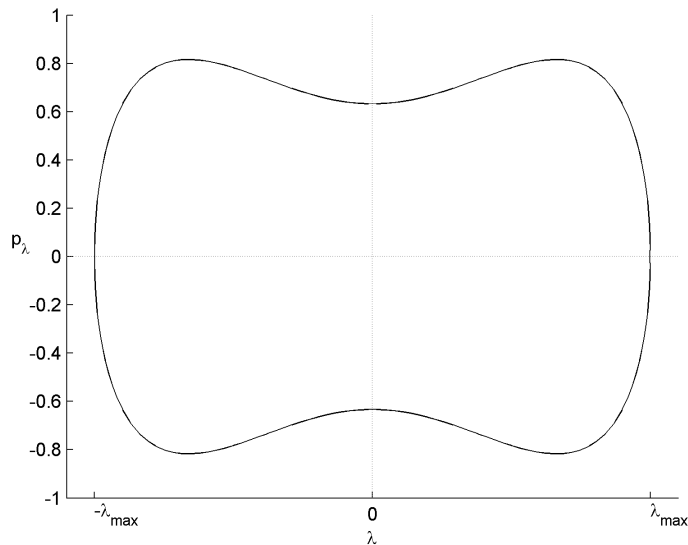


Figure 4: Phase diagram for λ with $(h, g) = (-0.3, 0.5)$ and $\mu = \frac{1}{3}$.

For I_ν , we calculate the integral $\int p_\nu d\nu$ from $\nu = -\pi$ to $\nu = \pi$, because this corresponds to a closed path. As depicted in figure 5, for lemniscate motion there are two possible cycles for any given h and g : one with positive and one with negative momentum. In the rest of this paper we will consider the case of positive p_ν , but all statements also hold for the reverse cycle.

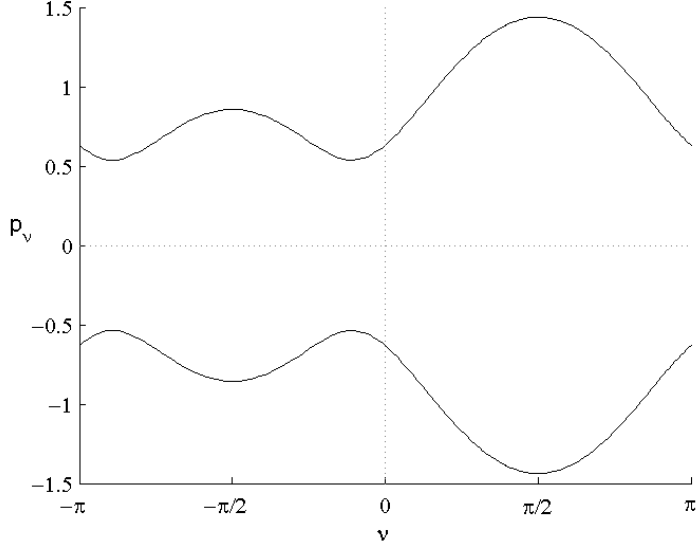


Figure 5: Phase diagram for ν with $(h, g) = (-0.5, 0.2)$ and $\mu = \frac{1}{3}$.

Looking at the phase diagram in figure 5 or at the corresponding equation (35), it can be seen that the part $\nu \in [0, \pi]$ has a symmetry around $\nu = \pi/2$. The same goes for the part $\nu \in [-\pi, 0]$ with a symmetry around $\nu = -\pi/2$. Therefore, instead of taking the integral of $p_\nu d\nu$ from $-\pi$ to π , we can take it from $-\pi/2$ to $\pi/2$ and double the outcome. So the action is

$$I_\nu = \frac{1}{\pi} \int_{-\pi/2}^{\pi/2} p_\nu d\nu. \quad (60)$$

4.2 Winding numbers

We define the winding W number as

$$W = \frac{\omega_\nu}{\omega_\lambda}, \quad (61)$$

where ω_ν and ω_λ are the frequencies of the motion in respectively the ν and the λ coordinate according to equation (56). If the winding number is a rational number $\frac{m}{n}$, with m and n coprime, m cycles in ν are completed in the time it takes to complete n cycles in λ . Or, stated otherwise: the total period T (the time to complete a full cycle) equals m times the period T_ν in ν and n times the period T_λ in λ :

$$W = \frac{m}{n} = \frac{T_\lambda}{T_\nu} \quad (62)$$

$$T = nT_\lambda = mT_\nu. \quad (63)$$

All periodic orbits have a rational winding number. The frequencies ω_ν and ω_λ depend only on h and g , and as a result so does W .

We are going to look for g for a given h and a desired W . We will do this using the actions I_λ and I_ν , which are independent functions of h and g : $I_\lambda = I_\lambda(h, g)$ and $I_\nu = I_\nu(h, g)$. These relations can be inverted to get $H(I_\lambda, I_\nu)$. We now use the fact

that H and G are independent constants of motion and thus that $\frac{dH}{dg} = 0$, to get a relation between W, I_λ, I_ν and g :

$$\begin{aligned}\frac{dH}{dg} &= \frac{\partial H}{\partial I_\lambda} \frac{\partial I_\lambda}{\partial g} + \frac{\partial H}{\partial I_\nu} \frac{\partial I_\nu}{\partial g} \\ &= \omega_\lambda \frac{\partial I_\lambda}{\partial g} + \omega_\nu \frac{\partial I_\nu}{\partial g} = 0\end{aligned}$$

so

$$W = \frac{\omega_\nu}{\omega_\lambda} = -\frac{\partial I_\lambda / \partial g}{\partial I_\nu / \partial g}. \quad (64)$$

Now we can use equations (59) and (60) for the actions and solve (64) for g .

We thus need to calculate the integrals $\frac{\partial}{\partial g} \int_0^{\lambda_{\max}} p_\lambda d\lambda$ and $\frac{\partial}{\partial g} \int_{-\pi/2}^{\pi/2} p_\nu d\nu$. For the latter, we can take the differentiation inside the integral:

$$\frac{\partial I_\nu}{\partial g} = \frac{1}{\pi} \int_{-\pi/2}^{\pi/2} \frac{\partial p_\nu}{\partial g} d\nu = \frac{1}{\pi} \int_{-\pi/2}^{\pi/2} \frac{g d\nu}{\sqrt{-2h \sin^2 \nu + 2(1 - 2\mu) \sin \nu + 2g}}. \quad (65)$$

For the λ -integral, though, the upper integration limit is dependent on g . However, we will show that in this case we can also take the differentiation inside the integral without changing the integration limits. For this purpose we introduce the notation $f(\lambda, g) = p_\lambda$ for the integrand, and $F(\lambda, g)$ for its antiderivative with respect to λ , so $f = \frac{\partial F}{\partial \lambda}$. We have

$$\begin{aligned}\frac{\partial}{\partial g} \int_0^{\lambda_{\max}} f(\lambda, g) d\lambda &= \frac{\partial}{\partial g} (F(\lambda_{\max}, g) - F(0, g)) \\ &= \left. \frac{\partial F(\lambda, g)}{\partial \lambda} \right|_{\lambda=\lambda_{\max}} \frac{\partial \lambda_{\max}}{\partial g} + \frac{\partial F(\lambda, g)}{\partial g} - \frac{\partial F(0, g)}{\partial g} \\ &= f(\lambda_{\max}, g) \frac{\partial \lambda_{\max}}{\partial g} + \int_0^{\lambda_{\max}} \frac{\partial f(\lambda, g)}{\partial g} d\lambda \\ &= \int_0^{\lambda_{\max}} \frac{\partial p_\lambda}{\partial g} d\lambda.\end{aligned}$$

The last step follows from $f(\lambda_{\max}, g) = 0$, which is how λ_{\max} is defined. We thus have

$$\frac{\partial I_\lambda}{\partial g} = \frac{2}{\pi} \int_0^{\lambda_{\max}} \frac{\partial p_\lambda}{\partial g} d\lambda = -\frac{2}{\pi} \int_0^{\lambda_{\max}} \frac{g d\lambda}{\sqrt{2h \cosh^2 \lambda + 2 \cosh \lambda - 2g}}. \quad (66)$$

Now we can substitute expressions (65) and (66) into expression (64) for the winding number, and solve numerically for g .

4.2.1 Elliptic Integrals

We can also express the elliptic integrals in (66) and (65) in algebraic form, when we substitute ξ and η for respectively λ and ν :

$$\frac{\partial I_\lambda}{\partial g} = -\frac{2}{\pi} \int_1^{\xi_{\max}} \frac{g d\xi}{\sqrt{(\xi^2 - 1)(2h\xi^2 + 2\xi - 2g)}}; \quad (67)$$

$$\frac{\partial I_\nu}{\partial g} = \frac{1}{\pi} \int_{-1}^1 \frac{g d\eta}{\sqrt{(1 - \eta^2)(-2h\eta^2 + 2(1 - 2\mu)\eta + 2g)}}. \quad (68)$$

The integrand in this last integral using η goes to infinity at the integration limits, which impairs the accuracy of numerical evaluation. The integrand using ν in equation (65) does not have this problem. It is therefore more advantageous to use the form in equation (65) for numerical evaluation.

For $\frac{\partial I_\nu}{\partial g}$ though, the integrand goes to infinity at the upper integration limit since this limit is a root of the denominator, regardless of whether we use λ or ξ . We can however express the integral in terms of Legendre's elliptic integral of the first kind.

To do this we first note that the zeros of the polynomial under the reciprocal square root in equation (67) are -1 , 1 , ξ_{\max} and ξ_0 , where ξ_{\max} is given by equation (51) and

$$\xi_0 = -\frac{1}{2h} - \sqrt{\frac{g}{h} + \frac{1}{4h^2}}. \quad (69)$$

For lemniscate motion, the order of these roots is

$$\xi_{\max} > 1 > \xi_0 > -1 \quad (70)$$

We now rewrite (51) as

$$\frac{\partial I_\lambda}{\partial g} = -\frac{2g}{\pi\sqrt{-2h}} \int_1^{\xi_{\max}} \frac{d\xi}{\sqrt{(\xi_{\max} - \xi)(\xi - 1)(\xi - \xi_0)(\xi + 1)}}, \quad (71)$$

which, according to relation **256.00** from [17], equals

$$\frac{\partial I_\lambda}{\partial g} = -\frac{2g}{\pi\sqrt{-h(\xi_{\max} - \xi_0)}} K\left(\frac{(\xi_{\max} - 1)(\xi_0 + 1)}{2(\xi_{\max} - \xi_0)}\right), \quad (72)$$

where $K(m)$ is Legendre's complete first integral with parameter m (which is the square of the elliptic modulus k). Evaluation of $K(m)$ can quite efficiently be done numerically (see, for example [18]) and is implemented in many software-packages, such as Matlab and Mathematica.

4.2.2 Finding W without using the Liouville-Arnold theorem

There is also another, arguably more intuitive, way of finding W in terms of h and g , that gives the same result as equation (64). We approach the problem by determining T_λ and T_ν , which are the times in τ needed to complete a full cycle in respectively λ and ν . This can be done by taking the integral of infinitesimal time steps over the whole cycle:

$$T_s = \oint d\tau, \quad (73)$$

where s can be either λ or ν . Now, $d\tau$ can be expressed as the travelled distance ds divided by the velocity $\frac{ds}{d\tau}$. From equations (26) and (28) we have $\frac{ds}{d\tau} = p_s$, so we get

$$T_s = \oint \frac{1}{p_s} ds. \quad (74)$$

For λ , the phase diagram is divided into four parts of same duration (figure 4), so:

$$T_\lambda = 4 \int_0^{\lambda_{\max}} \frac{1}{p_\lambda} d\lambda, \quad (75)$$

which is just $\frac{\partial I_\lambda}{\partial g}$ (equation (66)) times $-2\pi/g$. For ν , we have

$$T_\nu = \int_{-\pi}^{\pi} \frac{1}{p_\nu} d\nu = 2 \int_{-\pi/2}^{\pi/2} \frac{1}{p_\nu} d\nu, \quad (76)$$

which is $\frac{\partial I_\nu}{\partial g}$ (equation (65)) times $2\pi/g$. Now, using

$$W = \frac{T_\lambda}{T_\nu} \quad (77)$$

we get exactly the same expression as from equation (64).

4.2.3 Possible winding numbers

Figure 6 depicts the winding number W in the lemniscate region of the (h, g) -plane. For a given $h \in (h_{\min}, 0)$, $W(g)$ is a continuous strictly increasing function for g within this open region.

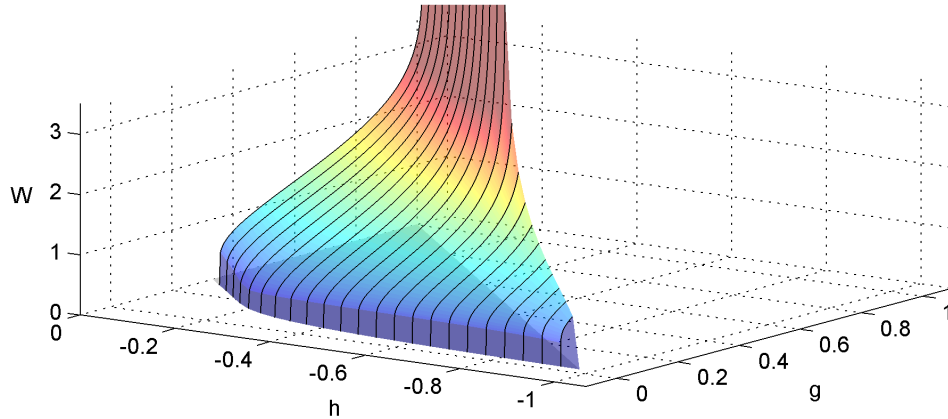


Figure 6: The winding number W as a function of h and g for lemniscate motion with $\mu = 1/3$. The domain is the region depicted in figure 3.

At the left boundary (small g , see figure 3) of the lemniscate region, T_ν is infinite while T_λ is finite, and therefore $W = T_\lambda/T_\nu$ is zero.

For the right boundary (large g), we can see in figure 6 that the winding number goes to infinity for sufficiently large h and remains finite for smaller h . Without

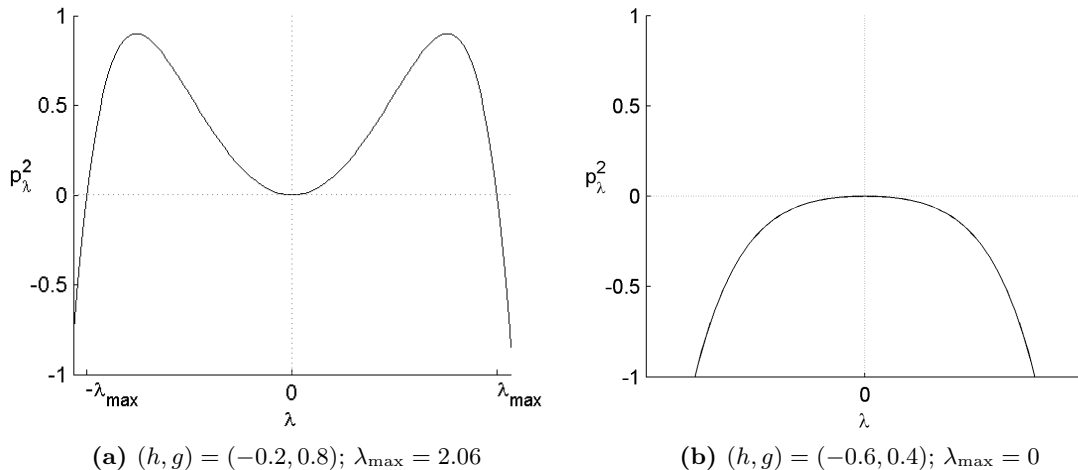


Figure 7: Phase diagrams for λ at the boundary of the lemniscate region. In (a) T_λ is infinite, while in (b) T_λ remains finite.

giving a rigid proof, we will argue that this transition occurs at $h = 0.5$. We will look at the polynomial on the right hand side of equation (34), where p_λ^2 is expressed in terms of λ . If this polynomial has a positive value for a certain value of λ , motion is physically allowed in an open interval around this value. At the right boundary of the lemniscate region, so where $g = h + 1$, the polynomial vanishes at $\lambda = 0$. Two examples are depicted in figure 7. We note that, since $p_\lambda^2(\lambda)$ is an even function, the zero at $\lambda = 0$ corresponds to either a local maximum or a local minimum.

When it is a local maximum (as in figure 7b), λ can only be zero, so there is no motion for the given h and g . We can determine if there is a local maximum by looking at the second derivative of $p_\lambda^2(\lambda)$:

$$\frac{d^2 p_\lambda^2}{d\lambda^2}(\lambda) = 4h(\sinh^2 \lambda + \cosh^2 \lambda) + 2 \cosh \lambda. \quad (78)$$

At $\lambda = 0$

$$\frac{d^2 p_\lambda^2}{d\lambda^2}(0) = 4h + 2, \quad (79)$$

which is negative for $h < -1/2$, meaning that there is a local maximum and thus that no motion in an open λ -interval is allowed. The physical reason that there is a zero at $\lambda = 0$ is that λ_{\max} vanishes. If for fixed $h < -1/2$ we approach the right boundary of the lemniscate region in the (h, g) -plane from the left, so by increasing g , oscillations in λ become smaller. The period T_λ remains finite. Therefore, for $h < -1/2$, also W remains does not go to infinity.

On the other side, when $h > -1/2$ the zero at $\lambda = 0$ is a local minimum and motion in an open λ -interval is allowed (see figure 7a). When we approach the right boundary of the lemniscate region from the left, the local minimum at $\lambda = 0$ lowers as g increases until it hits $p_\lambda^2 = 0$ at $g = h + 1$. Since motion slows down around $\lambda = 0$, the period T_λ increases. At the boundary $g = h + 1$, where there is a stationary point at $\lambda = 0$, T_λ is infinite. Therefore, W will go to infinity at the right boundary of the lemniscate region for $h > -1/2$.

So, for all fixed $h > -1/2$, $W(g)$ can take on any positive value in the lemniscate region. For fixed $h < 1/2$, $W(g)$ remains finite and is bounded above.

As we have seen in this section, there is a positive relation between the winding number and the value of the conserved quantity G . This gives us some grasp on the

physical meaning of G . A large winding numbers means that the frequency of the motion in ν is relatively large compared to the frequency of the motion in λ . Also, from equations (34) and (35), we see that the absolute rate of change in λ depends negatively on g , while there is a positive relation between the rate of change in ν and g . So, for larger g , the kinetic energy of the moving particle is more distributed in the ν direction and less in the λ direction. We can therefore consider G to be a measure of how much the orbits of the moving particle go “around” the two centers in contrast to being “in between” them.

5 Collisional orbits

Collisions occur whenever $(\lambda, \nu) = (0, \pm\frac{\pi}{2})$. At the collisions with the centers, λ changes sign, since $\lambda = 0$ and $p_\lambda \neq 0$. For lemniscate motion, the sign of p_ν is maintained along the whole orbit. Since λ changes sign and ν either decreases or increases at a passage through one of the centers, the moving particle reverses direction whenever a collision occurs. Furthermore, by symmetry of both p_λ and p_ν around respectively 0 and $\pm\frac{\pi}{2}$, the trajectory towards the center is completely retraced by the trajectory away from it in configuration space Q_2 .¹ Another way of explaining this retracing of the path is by time reversal symmetry: acceleration along a given trajectory is unaffected by time reversal. So when the moving particle reverses its direction of motion, it will retrace its own path.

In the following, we will look at collisional orbits for a given winding number $W = W(h, g)$. We do this by starting the motion at \mathbf{f}_1 or \mathbf{f}_2 and determine at what values of ν the orbit crosses the line $\lambda = 0$:

$$C_{h,\mu}^W = \{\nu \in [-\pi/2, \pi/2] \mid (0, \nu) \text{ is on a collisional orbit for given } W\}. \quad (80)$$

We only included ν in the range $[-\pi/2, \pi/2]$, because this describes all the points on the line $\lambda = 0$. Of course, $C_{h,\mu}^W$ always contains $-\pi/2$ and $\pi/2$, since these are the points of collision.

The remaining points $\{(0, \nu) \mid \nu \in [-\pi/2, \pi/2] \setminus C_{h,g}^W\}$ on the line $\lambda = 0$ all belong to non-collisional orbits. Since all lemniscate orbits cross the line $\lambda = 0$, this gives all non-collisional orbits of lemniscate type.

5.1 Irrational winding number

In the case of an irrational winding number W , the 2-torus formed by the angles ϕ_λ and ϕ_ν will be densely filled by the orbit of the moving particle. So as long as this torus contains one or both of the centers, the orbit will approach arbitrarily close to a collision. This certainly is the case for all values of h and g for which the generalized momenta p_λ and p_ν (equations (34) and (35)) are real at both centers, so for $h - 1 + \mu < g < h + 1$, which holds for all lemniscate motion. Therefore, all non-periodic lemniscate motion will approach both centers to a distance that is arbitrarily close to zero. In configuration space, the orbit will fill the inside of the ellipse formed by $\lambda = \lambda_{\max}$ (given by equation (52)).

5.2 Rational winding number

In the (λ, p_λ) phase plane (see figure 4), any trajectory has two symmetries: one around $\lambda = 0$ and one around $p_\lambda = 0$. Therefore, one whole cycle with duration

¹On the cylinder \bar{Q}_2 , the points of the trajectory towards a collision differs from those of the trajectory away from it. The second part of the collisional trajectory consists of the points in the (λ, ν) -plane that result from applying the transformation $(\lambda, \nu) \rightarrow (-\lambda, \pi - \nu)$ to the points on the first part.

T_λ can be divided into four parts, all of duration $T_\lambda/4$. The first part leads from $(\lambda, p_\lambda) = (0, p_\lambda^0)$ to $(\lambda_{max}, 0)$, the second part from $(\lambda_{max}, 0)$ to $(0, -p_\lambda^0)$, etcetera. This leads to the known values of λ as a function of τ/T_λ as shown in figure 8a.

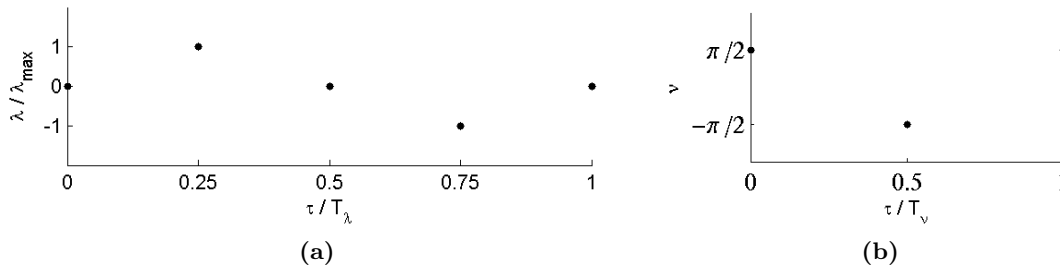


Figure 8: Known values for λ (a) and ν (b).

In the (ν, p_ν) phase plane (see figure 5), any trajectory has a symmetry around the line $\nu = \frac{\pi}{2}$ (or $\nu = -\frac{\pi}{2}$). So the whole period with length T_ν can be divided into two parts of duration $T_\nu/2$. One part leads from $\nu = \frac{\pi}{2}$ to $\nu = -\frac{\pi}{2}$ and the other one back to $\nu = \frac{\pi}{2}$. This is depicted in figure 8b.

So, by symmetry arguments, we know at what relative phase τ/T the path of the moving particle intersects with the lines $\lambda = 0$, $\nu = \frac{\pi}{2}$ and $\nu = -\frac{\pi}{2}$.

For example, consider the case of a collisional orbit with $W = 1$ in figure 9. When $W = 1$, $T_\lambda = T_\nu = T$. For non-collisional orbits, this corresponds to a figure-eight trajectory. We now consider the collisional orbit starting at \mathbf{f}_2 . At $\tau = \frac{1}{4}T$, $\lambda = \lambda_{max}$ and $\nu \in (\pi/2, \pi) \cup [-\pi, -\pi/2)$, which means that the free particle is somewhere on the ellipse $\lambda = \lambda_{max}$ at the left side of the z -axis. At $\tau = \frac{1}{2}T$, $\lambda = 0$ and $\nu = -\pi/2$, so there is a collision at \mathbf{f}_1 . As mentioned before, after a collision the free particle will retrace its own path in the configuration space Q_2 , but not on \bar{Q}_2 . At $\tau = \frac{3}{4}T$, $\lambda = -\lambda_{max}$ and $\nu \in (-\pi/2, \pi/2)$, the free particle is on the same point as at $\tau = \frac{1}{4}T$. At $\tau = T$, the free particle is back at \mathbf{f}_2 . The only crossings of the line $\lambda = 0$ occur at the centers, so $C_{h,\mu}^1 = \{-\pi/2, \pi/2\}$.

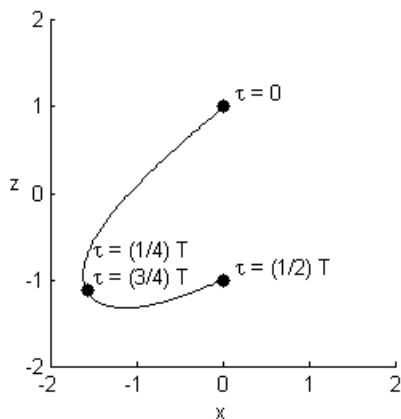


Figure 9: Orbit for $W = 1$, $h = -0.4$ and $\mu = 1/5$

We also note that for any rational winding number, all collisional orbits encounter exactly two collisions during a full cycle. This can be seen as follows. At every collision

²recall that we assumed p_ν to be positive

the free particle turns around and retraces its own trajectory. Therefore, if after a collision it encounters a second one, then it will follow its own path back and end up at the first collision again, completing a full cycle. So no more than two collisions are possible within one cycle. On the other hand, if a cycle is started at a collision, then at $\tau = T/2$, τ is an integer multiple of both $T_\lambda/2$ and $T_\nu/2$ and therefore the particle has to be at one of the centers. So there are at least two collisions in one cycle. This shows that there must be exactly two.

Case $W=m$

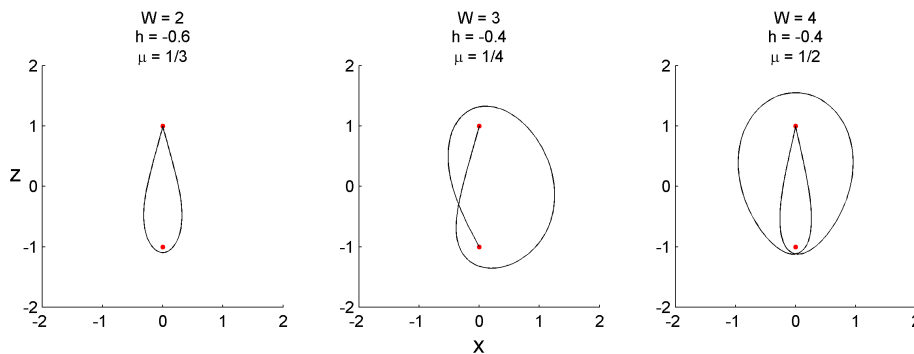


Figure 10: Examples of orbits with natural winding numbers

In the case of $W = m$, with m a natural number, T_λ is an integer multiple of T_ν . Some examples are depicted in figure 10. In this case, the free particle passes through m cycles in ν while completing one cycle in λ , and just so many half cycles of ν in one half cycle in λ . As discussed above, taking one of the centers $(\lambda, \nu) = (0, \pm\frac{\pi}{2})$ as initial position, any progression of τ by a multiple of $\frac{T_\nu}{2}$ will give $\nu = \pm\frac{\pi}{2}$ and the only passages of $\lambda = 0$ occur at multiples of $\frac{T_\lambda}{2}$. Since $\frac{T_\nu}{2}$ divides $\frac{T_\lambda}{2}$, all passages of $\lambda = 0$ will be at one of the centers. Therefore, any collisional orbit with $W = n \in \mathbb{N}$ will never pass the line $\lambda = 0$ connecting the two centers, other than at the endpoints, so we have:

$$C_{h,\mu}^m = \left\{ -\frac{\pi}{2}, \frac{\pi}{2} \right\}. \quad (81)$$

When $m \geq 2$, there are points on the trajectory of the free particle for which $\nu = \pm\pi/2$ while $\lambda \neq 0$, which correspond to points on the z -axis either below \mathbf{f}_1 or above \mathbf{f}_2 . For given m , the orbit will alternately cross below and above the two centers for a total of $m - 1$ times before there is another collision at $\tau = T/2$. This means that for odd m , the free particle will collide with both centers during one cycle. For even m , there are two collisions at the same center during one cycle, one after approaching from the left hand side of the (x, z) -plane and one from the right; the orbit will have a symmetry around the z -axis.

Case $W=1/n$

By the same reasoning as before, we can argue that for $W = 1/2$ the trajectory of the free particle crosses the line $\lambda = 0$ four times during one cycle: once at both centers ($\nu = \pm\frac{\pi}{2}$) and twice on some point on the line between the centers (dependent on the values of h and μ). For the general case $W = 1/n$, the collisional orbits go back and forth between the two centers, passing through a total of $n - 1$ distinct points on

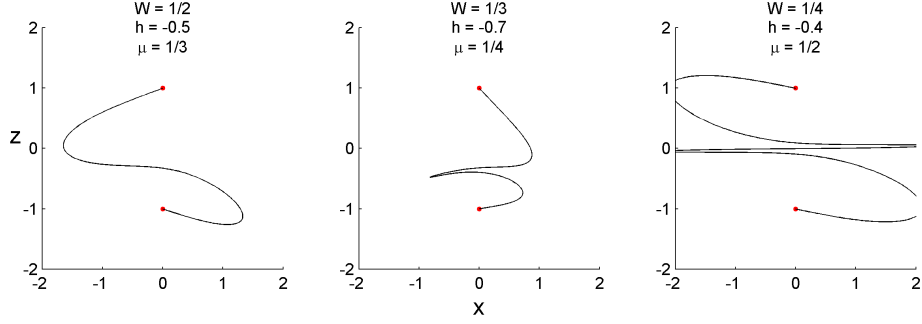


Figure 11: Examples of orbits with $W = 1/n$

the open-ended line between them, as can be seen in the examples in figure 11. We therefore have

$$C_{h,\mu}^{\frac{1}{n}} = \left\{ -\frac{\pi}{2}, c_1, c_2, \dots, c_{n-1}, \frac{\pi}{2} \right\} \quad c_i, \dots, c_i \in \left(-\frac{\pi}{2}, \frac{\pi}{2} \right). \quad (82)$$

For the case $\mu = 1/2$, the c_i 's lie symmetric around $\nu = 0$.

General rational winding number $W=m/n$

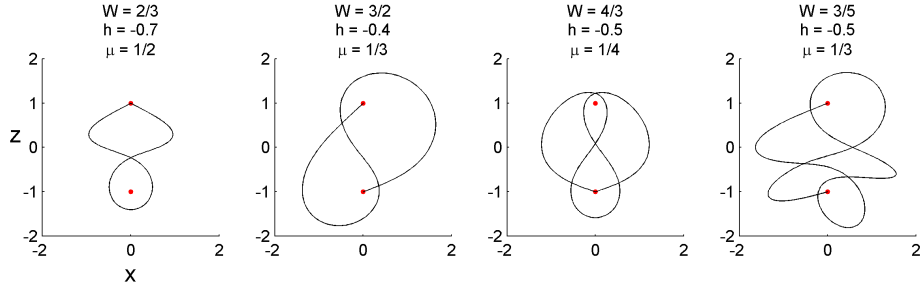


Figure 12: Examples of orbits with rational winding numbers

Examples of the general case $W = m/n$, with coprime $m, n \in \mathbb{N}$, are shown in figure 12. For this case the collisional orbits will cross the line $\lambda = 0$ a total of $2n$ times, of which two times at either one of the centers. These collisions are at the same center if m is even and at different centers if m is odd. The resulting $2n - 2$ intersections are generally at $n - 1$ different points, since the path from the first half of the orbit is retraced by the path from the second half. In the case of even m , the orbits will again be symmetric around the z -axis and as a result there are only $\frac{n-1}{2}$ distinct (non-collisional) points of intersection with the line $\lambda = 0$ in one orbit. However, since collisional orbits can start at either center, for even m there are two different collisional orbits, both with $\frac{n-1}{2}$ of non-collisional intersections with $\lambda = 0$. Thus we have, both for even and odd m :

$$C_{h,\mu}^{\frac{m}{n}} = \left\{ -\frac{\pi}{2}, c_1, c_2, \dots, c_{n-1}, \frac{\pi}{2} \right\} \quad c_1, \dots, c_n \in \left(-\frac{\pi}{2}, \frac{\pi}{2} \right), \quad (83)$$

with, for $\mu = 1/2$ and odd m again a symmetry around $\nu = 0$.

In conclusion, for any rational winding number $W = m/n$, there are n open intervals within $[-\pi/2, \pi/2]$ for which the orbits with initial condition $\lambda = 0$ and ν within this interval are non-collisional. Or, stated otherwise: there are n disjoint open intervals on the line $\{(x, z) \mid x = 0; z \in [-1, 1]\}$ that belong to non-collisional orbits and are separated only by points on this line.

6 Concluding remarks

We have shown that there are one-parameter families of non-collisional orbits in the two center problem. This means that there are non-collisional orbits for which a small change in the initial position will not lead to a collision, as long as the constants of motion remain unchanged. The one-parameter families can be represented by open intervals on the line segment connecting the two centers. These intervals are separated by points belonging to collisional orbits. Together, the intervals form a dense subset of the interval $[-1, 1]$, representing the line segment from one center to the other. We have however, not produced any general statements about the position of the points separating the intervals, which is something that might be looked at in the future.

To come to this result, we have taken a closer look at winding numbers for lemniscate motion and found that the range of possible winding numbers depend on the total energy of the system. For low energies, large winding numbers are not allowed. This makes sense, since at large winding numbers, the free particle moves around both centers many times before ‘collapsing’ through the line segment between them. This circling around requires a certain amount of energy.

In the current study, we only looked at lemniscate motion. The results might as well be extended to so-called satellite motion, for which the particle moves around only one of the centers. This requires some additional work, especially in calculating the winding numbers.

References

- [1] Carl Gustav Jakob Jacobi and Carl Wilhelm Borchardt. *Vorlesungen über dynamik*. G. Reimer, 1866.
- [2] Wolfgang Pauli. Über das modell des wasserstoffmolekülions. *Annalen der Physik*, 373(11):177–240, 1922.
- [3] Michael P Strand and William P Reinhardt. Semiclassical quantization of the low lying electronic states of H_2^+ . *The Journal of Chemical Physics*, 70:3812, 1979.
- [4] Mario M Jakas. Trapping of a classical electron between two heavy scattering centers. *Physical Review A*, 52:866–869, 1995.
- [5] Mario M Jakas. The production of high-energy electrons during low energy atomic collisions in solids. *Nuclear Instruments and Methods in Physics Research Section B: Beam Interactions with Materials and Atoms*, 115(1):255–260, 1996.
- [6] G Contopoulos. Periodic orbits and chaos around two black holes. *Proceedings of the Royal Society of London. Series A: Mathematical and Physical Sciences*, 431(1881):183–202, 1990.
- [7] G Contopoulos and H Papadaki. Newtonian and relativistic periodic orbits around two fixed black holes. *Celestial Mechanics and Dynamical Astronomy*, 55(1):47–85, 1993.
- [8] Holger Waalkens, Holger R. Dullin, and Peter H. Richter. The problem of two fixed centers: bifurcations, actions, monodromy. *Physica D: Nonlinear Phenomena*, 196(34):265 – 310, 2004.

- [9] Charles Alfred Coulson and Anthony Joseph. A constant of the motion for the two-centre Kepler problem. *International Journal of Quantum Chemistry*, 1(4):337–347, 1967.
- [10] Carl Vilhelm Ludwig Charlier. *Die Mechanik des Himmels*, volume 1. Veit, 1902.
- [11] A Deprit. Le problème des deux centres fixes. *Bull. Soc. Math. Belg*, 14(11):12–45, 1962.
- [12] TN Thiele. Recherches numériques concernant des solutions périodiques d’un cas spécial du problème des trois corps. *Astronomische Nachrichten*, 138(1):1–10, 1895.
- [13] Carl Burrau. *Über einige in Aussicht genommene Berechnungen betreffend einen Spezialfall des Dreikörper-Problems*. 1906.
- [14] Yiwu Duan and J-M Yuan. Periodic orbits of the hydrogen molecular ion. *The European Physical Journal D-Atomic, Molecular, Optical and Plasma Physics*, 6(3):319–326, 1999.
- [15] Jerry B. Marion and Stephen T. Thornton. *Classical Dynamics of Particles and Systems, fourth edition*. Saunders College Publishing, 1995.
- [16] Vladimir Igorevich Arnold. *Mathematical methods of classical mechanics, second edition*, volume 60. Springer, 1989.
- [17] Paul F Byrd and Morris D Friedman. *Handbook of elliptic integrals for engineers and physicists*, volume 67. Springer Berlin, 1954.
- [18] Roland Bulirsch. Numerical calculation of elliptic integrals and elliptic functions. *Numerische Mathematik*, 7(1):78–90, 1965.